FSO Transmission Link Performance Analysis for Enhancing Internet Infrastructure in Cote D'ivoire

Douatia Koné[1,2(✉)], Niangoran Medard Mené[1], and Aladji Kamagaté[1,3]

[1] Département Mathématiques-Physique-Chimie, Université Péléforo Gon Coulibaly, Korhogo, Côte d'Ivoire
douatiaben@gmail.com

[2] Direction de la Recherche et de l'Innovation Technologique, Ecole Supérieure Africaine des Technologies de l'Information et de la Communication, Abidjan, Côte d'Ivoire

[3] Département numérique et mathématiques, Agence National de Recherche, Paris, France

Abstract. Atmospheric free-space optical (FSO) transmission is one of the various types of wireless communication that are being developed today. This is an important alternative to consider for next-generation broadband to support high bandwidth. In this study we demonstrate the feasibility of using an FSO system in a 5G architecture operating in Côte d'Ivoire weather conditions, mainly in the following Korhogo, Man, Bouaké, Bondoukou, Man and Abidjan. Such an architecture requires high quality interconnection between the different parts of the network. To conduct this study, we collected meteorological data from January 2018 to December 2022 for each of these towns on the 'weather history' site. To characterize our propagation channel, we used the Gamma-gamma model. Attenuation levels caused by meteorological factors such as rain, fog, humidity and temperature were evaluated. Rain proved to be the most attenuating factor for FSO signals in Côte d'Ivoire, with attenuation levels of up to 5 dB/Km. The performance of these systems was analyzed in terms of signal-to-noise ratio and bit error rate. The results show that the rainy season is the least favorable time to deploy an FSO link, and that Man is the least favorable environment for such deployment. The Korhogo environment and the dry season are the most favorable for deploying an FSO connection. Similarly, for setting up an FSO connection, it is preferable to favor connection distances of less than 4.5 km.

Keywords: BER · FSO · Gamma-gamma distribution · SNR · Telecommunication · Côte d'Ivoire

1 Introduction

In an age of rapid digitalization and increasingly interconnected societies worldwide, the telecommunications play a fundamental role in the way we

A. Sere et al. (Eds.): AFRICOMM 2023, LNICST 587, pp. 133–154, 2025.
https://doi.org/10.1007/978-3-031-81570-6_9

communicate, share information and interact with our environment. However, behind the apparent ease of our telephone conversations, streaming videos, connected systems, autonomous vehicles and instantaneous messages, lie complex and profound issues that influence the way individuals, companies and nations are connected [1]. Particularly, Africa, as a continent undergoing rapid economic and digital growth, faces unique communication infrastructure challenges. Access to reliable broadband connectivity remains a major concern for many regions, due to geographical constraints, underdeveloped terrestrial infrastructures and the high costs associated with setting up traditional networks. According to a World Bank report, by 2021, 90% of the population in developed countries will have access to the Internet, while only 49% in developing countries [2]. Still according to the World Bank, in sub-Saharan Africa, only 36% of the population has Internet access, compared with 92% in North America, while in Côte d'Ivoire 45% of the population has Internet access. Innovative technologies are playing a crucial role in the search for solutions to bridge the digital divide. In this context, various systems are already in use in African states, notably in Côte d'Ivoire, where there are two main interconnection systems: wireless communication systems based on 3rd and 4th generation radio frequency (RF) technologies, and wired communication systems based on fiber optic technology [3]. Although these systems offer excellent performance, they are quite costly and difficult to deploy in certain regions due to the geographical profile of the area, especially in the case of fiber optics. Various technologies have been developed to overcome the limitations of existing technologies. Among these solutions, Free-Space Optics (FSO) technology is emerging as a promising alternative, capable of meeting connectivity needs at lower cost while overcoming traditional obstacles. By exploiting the fundamental principle of optical transmission through the free atmosphere, FSO systems promise high data rates on the order of fiber, low latency and rapid installation, making them an attractive solution for regions where the installation of wired infrastructure is difficult or impossible. Abu Jahid, Mohammed Alsharif and Trevor Hall present in a state-of-the-art analysis of FSO systems, the possibility of using FSO systems as a high-capacity backhaul connection system in 5th generation centralized architectures for the Internet of Things [4]. In [5], Yutao Shi and Al. present a method for improving the transmission capacity of a 5th generation network using a WDM-FSO interconnect. The main result of this work is to improve the mobility range of 5G wired and wireless communication systems through the joint use of the WDM-FSO link. However, changing weather conditions, such as heavy rainfall, high humidity, wide temperature variations and fog, can affect FSO signal quality, requiring sophisticated correction and attenuation mechanisms. Sherif Ghoname, Reba A. Fayed, Ahmed Abd EI Aziz, and Moustafa R. Aly have shown that humidity, fog and rain are important attenuation factors for the FSO link in Egypt. Their study shows that the attenuation levels caused by these factors can lead to a significant reduction in link margin for a transmission distance of 1 km [6]. It is in this context that a study carried out in Akure, Nigeria, presents the performance achieved by an FSO link in terms of link margin [7]. It shows that commercial systems operating at a wavelength of 1550 nm deliver excellent results in terms of link stability, with a link margin of over 0 dB for link distances of less than 10 km. In a previous study [8], it also analyzed the performance of a commercial FSO link operating at wavelength 1550 nm under Abidjan weather conditions. As a result, FSO systems could be perfectly deployed there, achieving excellent performance levels with BER of up to 10^{-13} for SNR values in excess of 50 dB.

In this paper, we aim to evaluate the influence of the meteorological seasons of a subtropical environment such as Côte d'Ivoire on the performance of a terrestrial FSO system, in particular for the environments of Korhogo, Man, Bouaké, Bondoukou, and Abidjan, which represent the main meteorological zones of Côte d'Ivoire. Mathematical models of the attenuation levels caused by rain, temperature, fog and humidity are analyzed and numerically simulated. Signal-to-noise ratio and bit error rate are considered as performance indicators, enabling a more general assessment of network link QoS. To characterize the turbulence of our propagation channel, we consider the Gamma-Gamma model [9], whose parameters are highly dependent on atmospheric and meteorological conditions [9,10]. Section 2 briefly describes the FSO technology and its modeling, while Sect. 3 discusses the influence of meteorological conditions on the FSO link. Section 4 presents the results combined with discussions and analyses. Section 5 concludes the paper.

2 FSO System for Telecommunication

FSO (Free Space Optics) systems are wireless communication technologies that use beams of light to transmit high-speed data through the open air, without the need for cables or physical wires. Unlike traditional technologies such as Wi-Fi, which use radio waves, FSO systems exploit light beams, usually in the visible light, infrared or mid-infrared range [11]. They operate between the 780 - 1600 nm wavelengths bands and use O/E and E/O converters. FSO systems work by using laser transmitters or LEDs to convert data into light signals. These light signals are then transmitted through the air to a remote receiver, where they are decoded into understandable data. These systems can be used for a wide range of applications, such as last-mile access in telecommunications networks where geographical conditions prevent the construction of a fiber-optic network. They can be used to link buildings or remote installations in urban or rural environments. Also, because of their independence from wired infrastructures, and ease of deployment, FSO systems can be used to rapidly restore communications in emergency situations when the fiber optic network fails, or the extension/development of an existing fiber optic network, or to provide high-speed connectivity for special events, trade fairs, etc. [12]. The main advantage of FSO systems is their ability to deliver very high data rates, ranging from several hundred megabits per second to several gigabits per second or even more, depending on conditions [13]. Because they use light rather than radio waves, FSO systems are not subject to electromagnetic interference from other wireless devices. Also, light beams are generally more difficult to intercept than radio signals, which can contribute to better data security [14]. The attractive features of FSO communications include licence-free operation, easy deployment which can be profitable for countries such as Côte d'Ivoire. Nevertheless, since their operating environment is the atmosphere, FSO systems can be affected by adverse weather conditions such as fog, rain, temperature, humidity or even air pollution. These factors can reduce the quality and range of the connection. So to determine their performances in a given environment, it's essential to understand the impact of each of these factors on the system, and to assess their intensity [9].

2.1 Network Architecture Design

Latest-generation communications network architectures are designed to meet the growing needs for connectivity, high throughput, low latency, and increased capacity. The fifth (5th) generation networks are also designed with this in mind. In order to provide efficient solutions to these needs and reduce deployment and operating costs, 5th generation networks rely heavily on network functions virtualization (NFV) and the decoupling of the control plane from the data plane. This enables network functions to be deployed and managed dynamically, allocating resources according to demand. This operating principle has given rise to a new, centralized architecture (called C-RAN for Cloud-Radio Access Network). In a C-RAN, the RAN's processing, control and management functions are centralized in a central data center (CU for centralized unit) or in network concentration points. Base stations (gNBs) in the field are reduced to relatively simple radio units (RUs), whose traffic management is handled by baseband units (BBUs) [14]. FSO technology is particularly well suited to this new network architecture, for the interconnection of RUs to the BBU (fronthaul connection), and/or as a secondary link for interconnection between the BBU and the CU (backhaul connection). Easy to deploy, it contributes in this architecture to reduce deployment and production time and costs, while enabling throughput levels of several Gigabytes per second [15]. Figure 1 shows a model of 5G architecture using FSO technology for the fronthaul interconnection and as a secondary link for the backhaul connection.

2.2 Analysis Method

When analyzing the performance of a telecommunication system, it is important to understand the intrinsic properties of its operating environment, in order to assess the level of losses the system may suffer as a result. For an FSO system, since the operating environment is the atmosphere, it is essential to model it accurately in order to assess its impact on system performance. The atmospheric channel is characterized by the presence of various meteorological factors (rain, fog, humidity, temperature) whose distribution varies over time. The method used to model our propagation environment must therefore be able to accurately describe the system's performance, taking into account the impact of these factors on it. Various propagation models exist for this purpose, but in

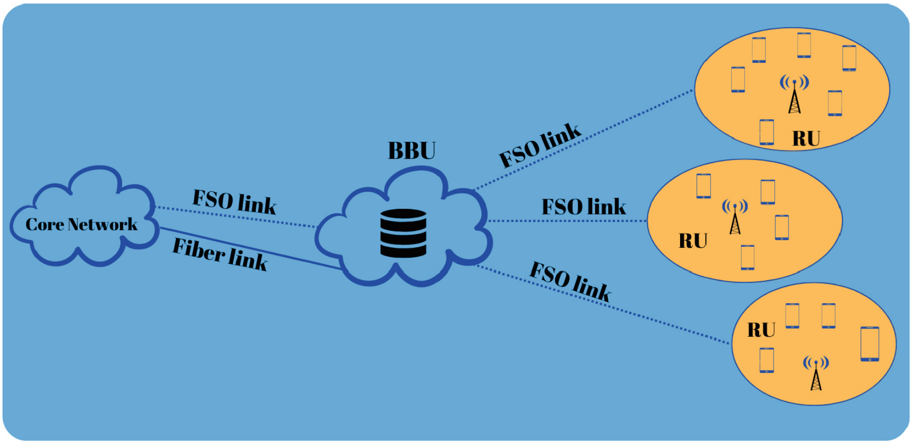

Fig. 1. 5G architecture using FSO technology for the fronthaul interconnection and as a secondary link for the backhaul connection

the FSO context the model generally considered is the gamma-gamma distribution model. The main advantage of this model is that it enables us to accurately describe the impact of atmospheric factors on the performance of an FSO system, whatever the nature (weak, medium, strong) of the atmospheric turbulence [16]. In this section we present the mathematical expression of this distribution and its role in the study of FSO system performance through the evaluation of SNR and BER.

2.3 Channel Modeling

Accurate modeling of the atmospheric channel in FSO systems is crucial for designing reliable links, estimating bit error rates (BER) and optimizing overall system performance for specific weather conditions. It is important to note that atmospheric channel modeling for FSO systems is often complex due to atmospheric variability and dynamics. Consequently, the used model must be capable of combining different parameters to account for the various physical phenomena involved in the propagation of optical signals in the atmosphere. In our case, in order to accurately account for the different scales of turbulence, we will use the gamma-gamma model. It can be used to describe atmospheric turbulence in low, moderate and high turbulence environments [17]. For this model, the distribution of irradiance as a function of atmospheric factors is given by Eq. 1 [17,18]:

$$\rho(I) = \frac{2(\alpha\beta)^{(\alpha+\beta)/2}}{\Gamma(\alpha)\Gamma(\beta)} I^{\frac{\alpha+\beta}{2}-1} K_{\alpha-\beta}(2\sqrt{\alpha\beta I}) \;, I\rangle 0 \tag{1}$$

K_v is the modified Bessel function of the second type, α and β are the effective numbers of small and large turbulence scales. The expressions for α and β are given by Eqs. 2 and 3 [18]:

$$\alpha = \left[exp\left(\frac{0.49\sigma^2}{1 + 1,11\sigma^{12/5}} \right)^{7/6} - 1 \right]^{-1}, \quad (2)$$

and

$$\beta = \left[exp\left(\frac{0.51\sigma^2}{1 + 0.69\sigma^{12/5}} \right)^{5/6} - 1 \right]^{-1}, \quad (3)$$

with σ^2 the atmospheric scintillation index, given by Eq. 4 [18,19]. For a horizontal link, the scintillation index is constant

$$\sigma^2 = 1,23 C_n^2 k^{7/6} L_p^{11/6}. \quad (4)$$

where Lp is the link length, k the wave number ($k = \frac{2\pi}{\lambda}$) and C_n^2 the refractive index structure parameter [19].

2.4 Signal-Noise-Ratio (SNR)

Signal-to-Noise Ratio (SNR) is an essential communications metric that evaluates the quality of the transmitted signal in relation to the level of noise present in the transmission channel. It is a fundamental measure used to evaluate the performance and reliability of communication systems [18]. Its expression is given by Eq. 5 [18],

$$\gamma = \frac{P_u}{P_n} = \frac{\eta I}{2\sqrt{N_0}} \quad (5)$$

where P_u and P_n are respectively the useful power and the noise power, η represents the optical to-electrical conversion coefficient, and N_0 the mean noise optical power. For reliable and efficient communication, it is important to maintain an adequate SNR, especially in wireless communication systems. SNR management and enhancement are important aspects of communication system design and performance optimization [18,20].

2.5 Bit Error Rate (BER)

BER (Bit Error Rate) is a measure of the quality of data transmission in a digital communication system. It represents the probability of data bits being received erroneously in relation to the total number of bits transmitted. It's important to note that BER is closely related to the signal-to-noise ratio (SNR) in a communication system. A higher SNR generally leads to a lower BER, as a stronger signal to noise ratio enables better detection and recovery of data bits. The expression of BER as a function of atmospheric parameters is given by Eq. 6 [18,20],

$$BER = \frac{1}{2} \int_0^{\infty} p(I) erfc\left(\frac{< SNR > (I)}{2\sqrt{2}} \right) \mathrm{d}I \quad (6)$$

where $erfc()$ is the complementary error function. To resolve this integral, the modified Bessel function of the second kind $K_v()$ in Eq. (1) is represented by the Meijer G function given by Eq. 7 [21]:

$$K_v = \frac{1}{2} G_{0,2}^{2,0}\left(\frac{x^2}{4}\middle|\begin{matrix} - \\ (v-2), -(v-2)\end{matrix}\right) \tag{7}$$

and the complementary error function $erfc()$ in Eq. (6) is represented by the Meijer G function given by Eq. 8 [22]:

$$erfc(\sqrt(x)) = \frac{1}{\sqrt{x}} G_{2,0}^{1,2}\left(x\middle|\begin{matrix} 1 \\ 0, 1/2\end{matrix}\right). \tag{8}$$

Replacing Eq. 1 by its expression in Eq. 6, and using the relations given in Eq. (7) and Eq. (8), as well as using the solutions of the resulting integral given [23], we obtain the closed-form expression of the BER given by Eq. 9:

$$\begin{aligned} BER = \tfrac{1}{2} - \tfrac{1}{4\sqrt{\pi}\alpha\beta\Gamma(\alpha)\Gamma(\beta)}\tfrac{\eta}{\sqrt{N_0}}\times \\ H_{1,3}^{3,2}\left(\left(\tfrac{\eta}{2\sqrt{N_0}\alpha\beta}\right)^2\middle|\begin{matrix}(\frac{1}{2},1),(-\alpha,2)(-\beta,2)\\(0,1),(-\frac{1}{2},1)\end{matrix}\right). \end{aligned} \tag{9}$$

2.6 Test Environment

Our operating environment Côte d'Ivoire. Côte d'Ivoire is a country with a surface area of 322,462 Km^2, and a population of 29,389,150. It is located in West Africa between the equator and the Tropic of Cancer. Côte d'Ivoire has a tropical climate, typical of the West African region. Because of its diverse geography, it has different climatic zones. The coast has an equatorial climate, while the interior of the country has a tropical climate with a rainy season and a dry season. The rainy season generally lasts from May to October. During this period, the country receives abundant rainfall, particularly in the south. July and August are often the wettest months. The dry season extends from November to April. During these months, the rainfall is much rarer, and the weather is generally warmer and drier. December to February are considered the driest months. Temperatures in Côte d'Ivoire vary according to region. In the coastal areas, temperatures are relatively moderate throughout the year, with averages around 25 to 30 °C (77 to 86 degrees Fahrenheit). In more inland and continental regions, temperatures can be higher, sometimes reaching 35 °C (95 degrees Fahrenheit) during the hot season [24]. Figure 2 shows the climate map of Côte d'Ivoire. In order to study the feasibility of deploying an FSO link to provide telecoms services in this environment, we consider five cities that perfectly represent the different meteorological characteristics of Côte d'Ivoire. The chosen cities chosen are Korhogo, Bouaké, Abidjan, Man and Bondoukou. For each of these cities, metrological data from 2018 to 2022 were obtained from the "weather-history" platform [25]. The analyzed parameters are visibility, temperature, humidity and precipitation data per hour. The values of these parameters were collected from the “weather history” platform. For our simulations, we considered a system operating at a wavelength of 1550 nm, as this is the wavelength commonly used in commercial FSO systems [17]. Numerical simulations of our system’s performance are carried out using *MATLAB* software.

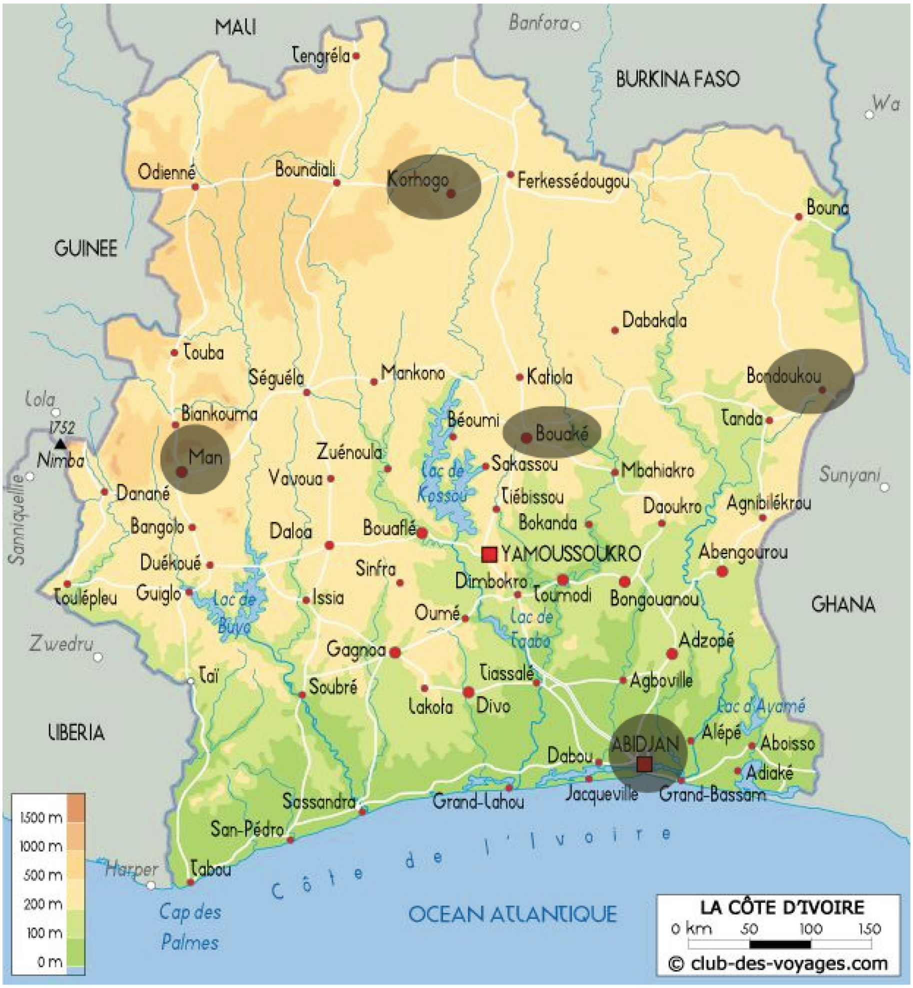

Fig. 2. Climatic map of Côte d’Ivoire

Korhogo in terms of population, Korhogo is the fourth most populous city in Côte d’Ivoire, and the largest city in the north of the country, with a population of 243,048 inhabitants in 2021 [26]. The climate is Sudanese (very hot and very dry). The climate is characterized by two main seasons. The long dry season from October to May precedes the rainy season marked by two rainfall peaks, one in June and the other in September. The December and January periods are marked by the harmattan, which causes temperatures to drop sharply. Korhogo is located at 380 m above sea level, with an average visibility distance of 10 Km [25].

Bouaké is Côte d'Ivoire second most populous city in terms with 536,719 inhabitants in 2021 [26], it covers an area of 72 Km^2. Bouaké has a tropical climate, with two main seasons: the rainy season from May to November and the dry season from November to May. This environment is located at 312 m above sea level, in the center of Côte d'Ivoire and has an average visibility range of 10 Km [25].

Abidjan is the largest city in Côte d'Ivoire in terms of population and surface area. It has a population of around 5 million inhabitants for a surface area of 422 Km^2 in 2021 [26]. In terms of climate, Abidjan enjoys an sub-equatorial climate, hot and humid. The rainfall is abundant over 1441 mm of water per year. This environment is located at 18 m above sea level in southern Côte d'Ivoire, on the shores of the Gulf of Guinea. It has an average visibility range of 10 Km [25].

Man is a large city in western Côte d'Ivoire and the capital of the Tonkpi region. It borders Liberia and has a population of around 200,000 inhabitants in 2021 [26] for a surface area of 64 Km^2. Man has a savannah climate with dry winters (Aw) according to the Koppen-Geiger classification. The average temperature in Man is 25°C and rainfall averages 1569 mm annually. This environment is located at 329 m above sea level. It has an average visibility range of 9 Km [25].

Bondoukou is a town in the north-east of Côte d'Ivoire, capital of the Gontougo administrative region of Gontougo, close to Ghana. It has a population of over 78000 inhabitants [26]. In Bondoukou, the rainy season is oppressive and cloudy. the dry season is humid and partly cloudy, and the climate is hot all year round. This environment is located at 343 m above sea level. It has an average visibility distance of 10 Km [25].

3 Weather Influence on FSO Link

3.1 Rain Influence on FSO Link

The rain is a meteorological phenomenon that occurs when water condensed in the atmosphere falls back onto the Earth's surface in the form of liquid water droplets. Rain generally occurs when warm, moist air rises into the atmosphere and cools, causing water vapour to condense into water droplets. These droplets then clump together to form water-laden clouds, and when they become heavy enough, they fall to the ground as rain. Raindrops cause scattering independent of the wavelength of the light beam; rain is said to be a non-selective scattering factor. According to ITU-R recommendations, the attenuation caused by rain in a given environment is described by Eq. 10 [25]

$$\beta_{pluie} = \alpha R^{\rho}. \tag{10}$$

The values of α and ρ depend on the precipitation rate per hour of the test environment. For an environment like Côte d'Ivoire where R<3.8 mm/h [23,24], we have $\alpha = 0.509$ and $\rho = 0.63$ [18,26].

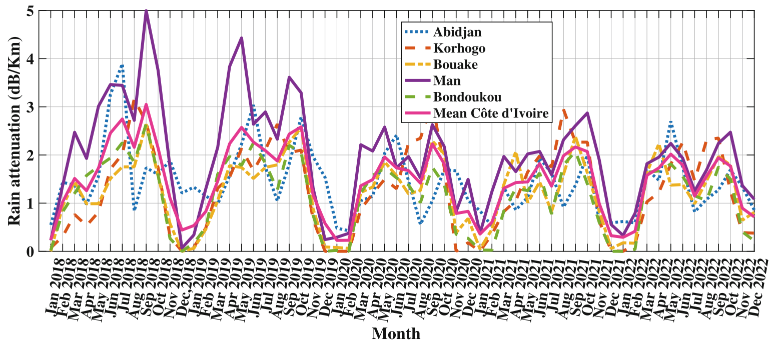

Fig. 3. Rain attenuation of the FSO link per month

Figure 3 shows the levels of rain attenuation per month on an FSO link from 2018 to 2022 in Abidjan, Bondoukou, Bouaké, Korhogo, and Man. The simulation parameter is the average precipitation rate per hour. For each of our test areas, its values have been collected on the "weather history" platform. The collected values are from 2018 to 2022. In general, the curves shown in Fig. 3 have the same appearance. They are characterized by two main trends. They show peak attenuations during the rainy season, mainly in July, August and September, followed by low attenuations during the dry season, especially in November, December and January. The Figure also shows that the environment with the highest rain attenuation is Man, with levels above the national average. The rainy season lasts an average of 9 months (February to November) in this environment. In 2018 and 2019, rain attenuation reached a maximum value of 5 dB/Km during the rainy season, compared with 3 dB/Km for the national average. Over the past three years, rain attenuation has decreased and now reaches a maximum value of 3 dB/Km. This can be explained by the decrease in rainfall due to climate change observed over this period. Maximum attenuations are observed during the months of May and September, which correspond in this area to the months with the highest rainfall rates [24,27]. Abidjan is the second environment where rain attenuation is the highest during the rainy season. Its attenuation levels are generally lower than the national average, except in the high rainy season where they reach a maximum value of 2.6 dB/Km observed during the period from May to July [28]. In Korhogo, Bondoukou and Bouaké, attenuations are below the national average, except during the peak rainy season (July-August-September), where peak attenuations in Korhogo are above the national average. In the dry season, rain attenuation tends towards 0 in each of our environments. This is explained by the scarcity of rainfall during this period [25,28]. These attenuation values are relatively low enough to block the FSO link in the context of telecommunication transmission for internet access [29]. Indeed, for an Internet connection, the recommended attenuation levels are those below 30 dB. So, in view of the overall attenuation levels observed, our test areas are excellent candidates for the deployment of an internet network using FSO technology [29].

3.2 Fog Influence on FSO Link

Fog is a meteorological phenomenon that occurs when small droplets of water suspended in the air reduce visibility at the Earth's surface. Fog generally forms when the air cools and its ability to retain moisture diminishes, causing water vapour to condense into tiny droplets [30]. The fog-forming process is often linked to specific weather conditions, notably night-time cooling and high humidity. When fog is dense, airborne water particles can scatter and disperse light from the optical beam, resulting in signal attenuation. Fog can act as an obstacle to optical beams, reducing the range and quality of transmission in an FSO system. The effects of fog on an FSO system depend on the intensity of the fog, the wavelength of the used optical beam, and the optical properties of the fog itself - fog is said to be a selective attenuating factor. Under conditions of intense fog, FSO transmission can become very limited, if not impossible. Equation 11 describes the attenuation caused by fog on a bond defined from Kim's experimental model for Mie scattering [30,31]

$$\beta_{brouillard} = \frac{3.91}{V}\left(\frac{\lambda}{\lambda_0}\right)^{-p}. \tag{11}$$

where V (Km) is the transmission distance, $\lambda_0 = 550\,\mathrm{nm}$ is the visibility range reference wavelength, λ (nm) is the wavelength used for interconnection and p is the particle size distribution coefficient. The values of p described by the Kim model are given by Eq. 12 [18,30]

$$p = \left\{\begin{matrix} 1.6 & ,V\rangle 50 \\ 1.3 & ,6\langle V\langle 50 \\ 0.16V + 0.34 & ,1\langle V\langle 6 \\ V - 0.5 & ,0.5\langle V\langle 1 \\ 0 & ,V\langle 0.5 \end{matrix}\right\}. \tag{12}$$

Figures 4 and 5 show the attenuation levels experienced by an FSO link in Abidjan, Bondoukou, Bouaké, Korhogo and Man, respectively, as a function of line-of-sight distance and month. For our simulations, we considered a transmitter using the 1550 nm wavelength, because it is more resistant to atmospheric attenuation factors than lower wavelengths. The simulation parameter is the average monthly variation in visibility distance. Its values were obtained from the "weather history" platform [25]. Figure 4 shows that the attenuation curves due to visibility distance for each of our test zones overlap. This reflects the small variation in sight distance between these zones. Overall, the levels of sight distance attenuation observed are low. The other main finding is that sight distance

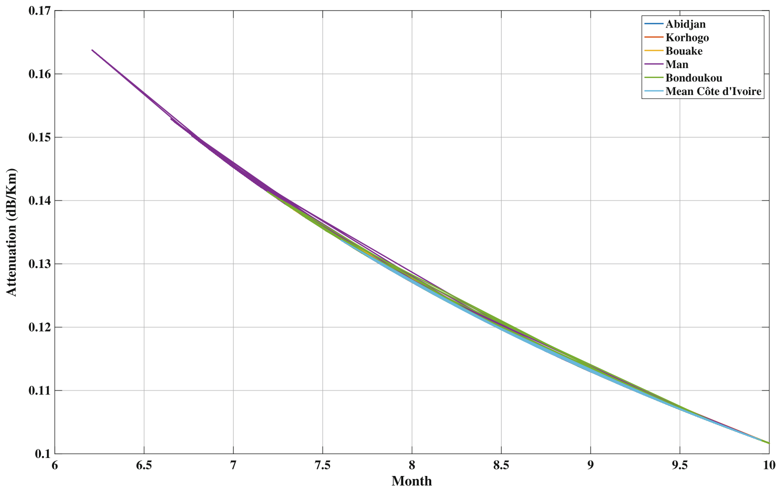

Fig. 4. Attenuation due to fog as a function of visibility distance

attenuation decreases as sight distance increases. With a visibility distance that can drop to 6.2 Km at an attenuation of 0.163 dB/Km, Man is the area with the lowest visibility distance and the highest level of sight distance attenuation. This might be due to the area's heavy rainfall and mountainous profile. These attenuation levels are relatively low enough to completely block the link in the case of Internet data transmission [29,32].

In order to assess the monthly attenuation caused by fog on the FSO link in the Korhogo, Bouaké, Abidjan, Man and Bondoukou areas, we considered the average variation in visibility distance from January 2018 to December 2022 in each of our test areas as a simulation parameter. Numerical simulation of the attenuation caused during the month by fog is carried out using MATLAB numerical simulation software. Figure 5 shows the monthly attenuation curves caused by fog from January 2018 to December 2022. These curves have the same appearance as those in Fig. 3, which show the evolution of rain attenuation curves. In fact, as in Fig. 3, the curves shown in Fig. 5 have two general trends over the entire analysis period. High attenuation is observed during the rainy season (May to October) and low attenuation during the dry season, mainly from November to January. These observations reflect the important role played by rain in reducing visibility distance in our test area. The Man zone is the area with the highest levels of fog-induced attenuation. Fog-induced attenuation in this environment remains above the national average throughout the analysis period. In this environment, peak attenuation of 0.16 dB/Km is observed during August and September 2018. From 2019 onwards the peak value of attenuation due to fog drops to around 0.15 dB/Km, which can be explained by the lower monthly rainfall observed from this year onwards [27]. Contrary to the observation made for rain attenuation, the second zones with the highest fog attenuation

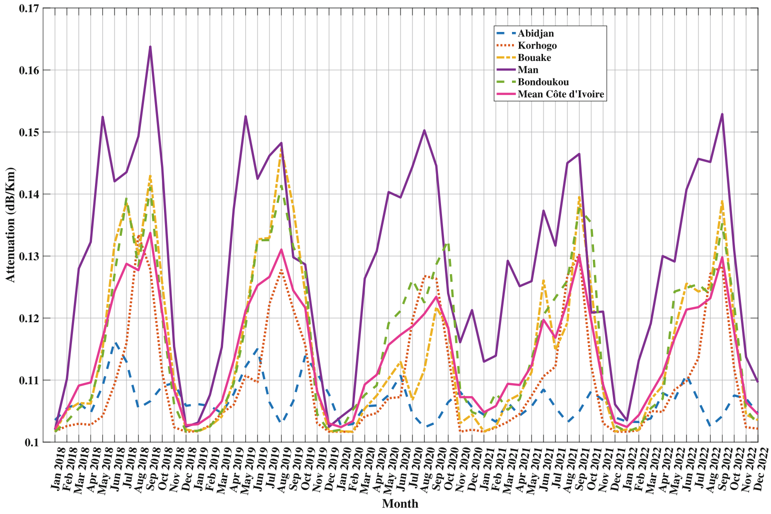

Fig. 5. Fog-induced attenuation of the FSO link for the wavelength 1550 nm

are Bouaké and Bondoukou, whose curves seem to overlap. This time, Korhogo and Abidjan have attenuation values below the national average. Bondoukou and Bouaké record attenuation peaks of around 0.142 dB/ Km during periods of heavy rain (August and September) [25]. This change in the ranking of cities with the highest attenuation is due to the fact that the presence of rain in some cases can reduce fog formation. Fog forms when the air is saturated with water vapor and cooled, causing moisture to condense into water droplets. When it rains heavily, the air is already saturated with moisture due to the rain, which means there is less potential for the additional condensation required to form fog droplets [33]. The Korhogo and Abidjan environments record levels of fog attenuation below the average trend. During the dry season, fog attenuation drops to around 0.1 dB/Km. The observed fog-induced attenuation and visibility values are low enough to prevent FSO transmission from working properly in these areas as part of the deployment of a fronthaul network for Internet access [14, 29].

3.3 Humidity Attenuation

Atmospheric humidity can also have an impact on free-space optical communication (FSO) systems. When humidity is high, the atmosphere contains a greater quantity of water vapor, which can lead to the absorption of infrared (IR) light used in FSO systems. Absorption of IR light by humidity can lead to attenuation of the optical signal, reducing the range and reliability of FSO communication [30]. In addition to light absorption, humidity can also lead to the formation of airborne water droplets, which act as obstacles to the optical beam. These droplets can scatter light and cause signal dispersion, resulting in fluctuations in the power of the optical signal received [29,32]. Equation 13 describes the absorption levels caused by humidity [30]

$$\left\{ \begin{array}{ll} \sigma = e^{-A_i \times w^{1/2}} & \text{Si } w < w_i \\ \sigma = k_i \left(\frac{w_i}{w}\right) \beta_i & \text{Si } w > w_i \end{array} \right\}. \tag{13}$$

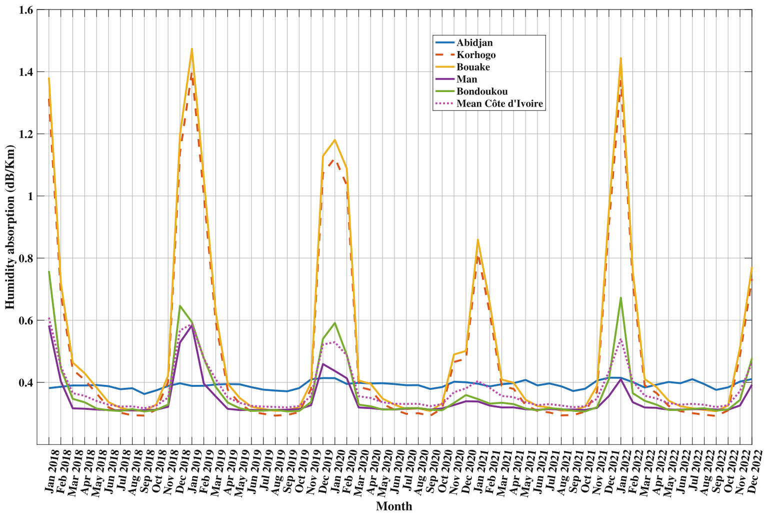

Fig. 6. Humidity-induced attenuation of the FSO link

With $\beta_i = 0.111$, $w_i = 1.1$, $k_i = 0.802$ and $w = \frac{1}{\rho_w} \int_{z_{sol}}^{z_t} \rho \times q_v \, dz$ the amount of precipitable water in the atmosphere. Figure 6 shows the monthly attenuation levels caused by fog in each of our test areas. To obtain it, we considered as simulation parameter the monthly specific humidity in Abidjan, Bondoukou, Bouaké, Korhogo, and Man. Its values from January 2018 to December 2022 were collected on the "historical-meteo" platform [25]. Our numerical simulations were carried out using Matlab. Generally speaking, the moisture attenuation curves for each of our environments follow the same pattern throughout the study period. For the Bondoukou, Bouaké, Korhogo and Man zones, two main trends are observed. We observe a period of low attenuation corresponding to the rainy season (May to October) and a period of high attenuation observed during the dry season, especially during the harmattan (November to March) [25]. This result can be explained by the fact that this period is characterized by a peak in specific humidity, mainly due to a sudden change in temperature between night and day. Indeed, it's very cold at night, but very hot during the day [25]. Humidity levels encountered during this period are generally of the order of 62% and are not high enough to lead to the formation of large raindrops. The particles thus present in the atmosphere are not dissipated by precipitation. This increases the water content of the atmosphere, resulting in high levels of specific moisture attenuation. The areas with the highest levels of attenuation, with peaks of around 1.4 dB/Km, are those of Korhogo and Bouaké, which are areas where harmattan is generally the most pronounced [34]. This value, higher than the national average of around 0.6 dB/Km, is observed during the month of January, which corresponds to the month of peak harmattan winds [25]. The Bondoukou area has the second highest attenuation levels, with peaks of around 0.6 dB/Km, again observed in January. It is followed by Man, which shows the same trends. As for the Abidjan area, attenuation levels vary slightly from month to month. Attenuation values in this zone seem constant at 0.4 dB/Km. This can be explained by the absence of harmattan winds in the south. As the Abidjan and Man zones are the ones with the most overcast periods during the year, humidity tends to be dispersed by rain, reducing its impact in terms of specific attenuation. During the rainy season, a sharp drop in attenuation due to specific humidity is observed in Bondoukou, Bouaké, Korhogo and Man. In Abidjan, the drop remains relatively small. This is explained by a balance in water content over the year, mainly due to evaporation of seawater. Overall, the attenuation levels observed, being well below 30 dB, should not prevent the FSO link from operating smoothly in our test areas as part of the deployment of a fronthaul network for Internet access [14,29].

3.4 Temperature Attenuation

Atmospheric temperature can have an impact on free-space optical communication (FSO) systems. As the temperature rises, the ambient air heats up, which can lead to variations in air density and refractive index. These variations in refractive index can deflect the optical beam, resulting in light scattering and optical signal degradation. This phenomenon is known as atmospheric turbulence and can be characterized by the Richardson number (Ri), a parameter used to characterize atmospheric stability conditions as a function of vertical wind speed gradient and thermal stratification. For values of R_i below the threshold of 1, the environment is said to be unstably stratified (presence of cells with strong turbulence); for R_i above 1, the environment is said to be stably stratified (presence of cells with weak turbulence) [35]. Equation 14 illustrates its expression [35,36].

$$R_i = \frac{g\beta \bigtriangleup T L_c}{v^2}. \tag{14}$$

where β is the coefficient of thermal expansion $[K^{-1}]$, $\triangle T$ is the temperature difference between the hot wall temperature T_c and the reference temperature T_r [K], L_c is the characteristic length [m], and v is the fluid speed [m/s].

Figure 6 shows the variation in Richardson number over time for each of our test areas. To obtain it, we used as simulation variables the monthly temperature from January 2018 to December 2022 for Korhogo, Bouaké, Abidjan, Man, Bondoukou. The mathematical expression of the richardson number was numerically simulated using the $MATLAB$ system. The results described in Fig. 6

show that in each of our zones the Richardson number varies between 2.4 and 4. The Richardson number is a ratio between the stabilizing force due to thermal stratification and the destabilizing force due to vertical wind shear. When R_i is above a certain critical threshold of 1, the atmosphere is considered stable, i.e. thermal stratification predominates and there is little turbulence. Also, the values of R_i observed in our test zones suggest that they are zones of stable stratification [34,35]. The zones in which we observe the highest levels of R_i are Bondoukou, Bouaké and Korhogo, which correspond to the zones with the lowest attenuation amplitudes on the FSO link. These zones have their R_i above the mean value. The Man and Abidjan zones have the lowest R_i values, with levels below the national average. The best R_i values are observed during the dry season (November to April), which justifies the low attenuation values observed during this period. The low levels of R_i observed during the rainy season allow it to retain its status as the least favorable season to the operation of the FSO link. As our study areas are low-turbulence zones, it is possible to deploy an FSO link there as part of the establishment of an Internet network in these areas [17].

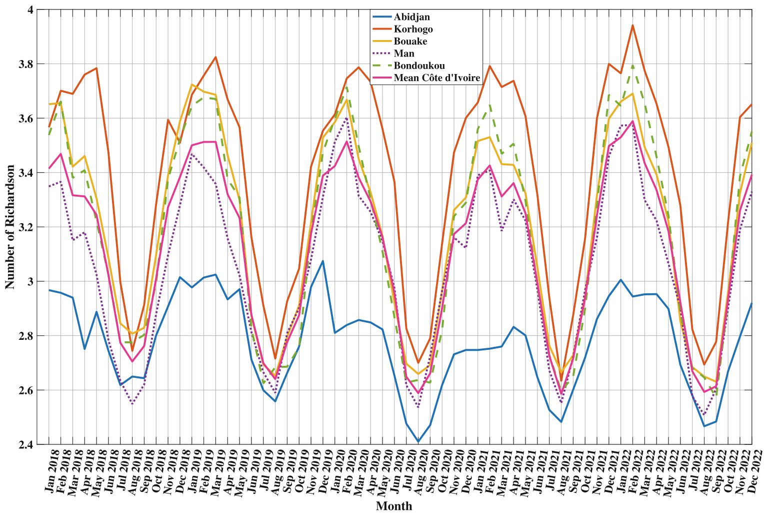

Fig. 7. Temperature-induced attenuation of the FSO link

4 Analysis and Discussions

4.1 Analysis

This section is devoted to analyzing the system's performance under the specific meteorological conditions of Korhogo, Bouaké, Bondoukou, Man and Abidjan. To do so, we analyze the values of the signal-to-noise ratio as a function of the transmission distance, and those of the bit error rate as a function of the signal-to-noise ratio. We use $MATLAB$ as our numerical simulation software. Simulation parameter values are given in Table 1.

Table 1. Operating parameters of FSO system

Operating parameters	Value
Transmitter Power	0.16 mW
Transmitter Efficiency	0.9
Receiver Efficiency	0.9
Wavelength	1550 nm
Electrical Bandwidth	1 Ghz
Laser Beam Divergence Angle	1 mrad
PIN Load Resistance	1 $K\Omega$
Dark Current	10 nA
PIN Responsivity	0.6 A/W

– **SNR vs Range**

The signal-to-noise ratio (SNR) is an essential indicator of link performance, giving us an idea of the quality of the received signal. For a transmitted signal operating at a wavelength of 1550 nm, at a transmit power of 0.1 dB and modulated according to the OOK-NRZ modulation scheme under the meteorological conditions of the selected areas, we obtain the results presented in Fig. 7, which shows the SNR variations as a function of the transmission distance of our FSO link. Figure 7 shows that the average SNR value evolves inversely with the link distance for each of our selected zones. For FSO link distances of less than 1 km, the SNR value varies between 170 dB and 50 dB. This indicates a good link quality for these transmission distances. For the FSO link distances between 1 Km and 4.5 Km, our environments maintain good SNR values, with a minimum value of 20 dB observed at Man. Beyond 4.5 Km, SNR values for Man fall below 20 dB, then to around 2 dB for a link distance of 10 Km, making Man the least favorable environment for FSO link deployment in terms of performance. The Abidjan, Bouaké and Bondoukou areas maintain SNR levels above 20 dB for a link distance of 6 Km. Korhogo, maintains SNR levels above 20 dB for link distances of up to 10 km. Korhogo is therefore the most favorable environment for deploying an FSO link. In view of these results, for the deployment of an FSO link in the general meteorological conditions of Côte d'Ivoire, distances less than 4.5 km should be favored. Indeed, for distances of less than 4.5 km, the link maintains the minimum 20 dB threshold required to establish a good Internet connection [37].

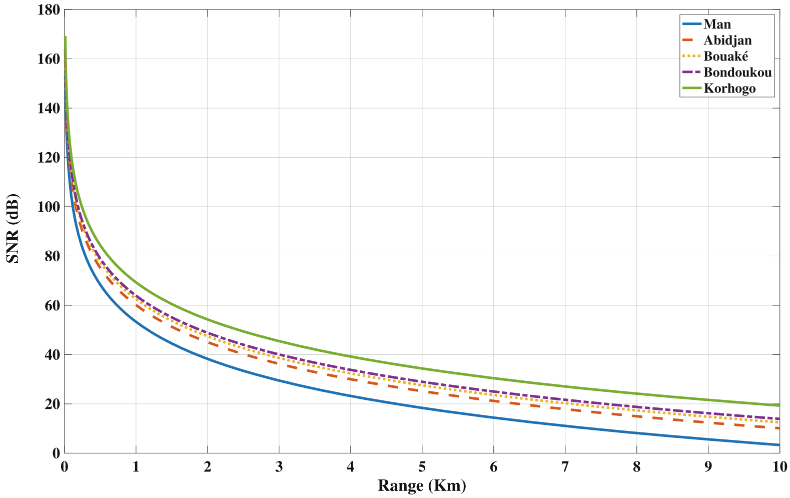

Fig. 8. SNR vs Range

– **BER vs SNR**

In order to evaluate the bit error rate (BER) of our system, we consider a signal modulated according to the On Off Keying Non-Return-to-Zero (OOK-NRZ) modulation scheme with a raised cosine impulse response filter [16] in the presence of atmospheric turbulence caused by weather conditions in Korhogo, Bouaké, Bondoukou, Abidjan, and Man. The BER values are shown in Fig. 9. Figure 9 shows the evolution of BER as a function of SNR in the meteorological conditions of Bouaké, Bondoukou, Man, Korhogo and Abidjan. The general shape of the curves shows that the BER decreases with increasing SNR. It shows that the highest value of the bit error rate for the FSO link in the general Ivorian meteorological context is observed in the Man area, and is of the order of 10^{-3}. This value is reached for an SNR value of 50 dB. This indicates fairly poor link performance in this environment. As BER is also dependent on atmospheric factors, these results could be explained by the high levels of attenuation observed in this environment. According to ITU-R S.579, atmospheric attenuation leads to an increase in BER through the induction of unwanted noise [38]. For a good link performance in telecommunication applications, we would need to find a method of reducing this value to at least 10^{-6} [39]. As for the Korhogo environment, it presents the best results in terms of BER, with values below 10^{-6} for SNR values above 20 dB, this can be explained by the low levels of attenuation observed in this environment. This suggests that the FSO link could be deployed for Internet telecoms applications in this area [39]. The Abidjan, Bouaké and Bondoukou environments show minimum BER values between 10^{-5} and 10^{-6} for SNR values between 35 dB and 50 dB. This also reflects the deployment potential of the FSO link for Internet telecommunication applications in this area [40]. In

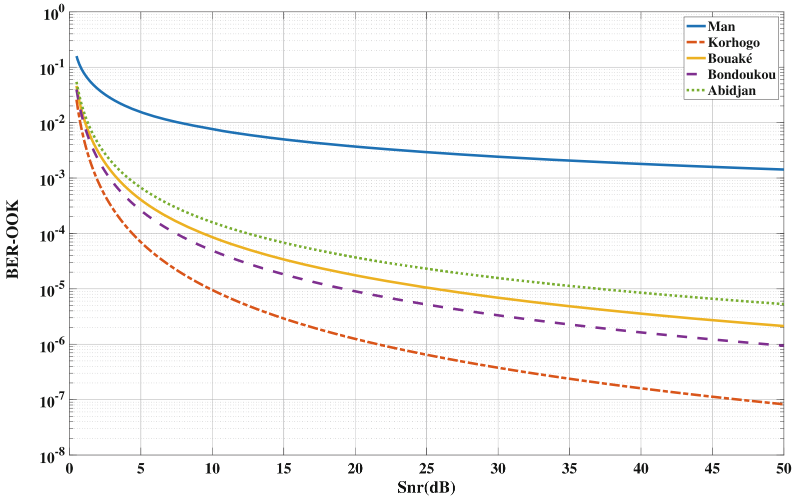

Fig. 9. BER vs SNR

view of this figure, Korhogo appears to be the most favorable environment for the deployment of an FSO link in Côte d'Ivoire, and Man the least favorable. Our results also show that for the use of an FSO system in our test areas as part of a Fronthaul interconnection for 5th generation networks, it is essential to integrate an autonomous error correction system into our architecture.

4.2 Discussion

It's worth pointing out that, compared with other contexts such as South Africa, where FSO technology has been used, Côte d'Ivoire has less restrictive characteristics for the connection. Indeed, in this environment, attenuation can reach 60 dB/Km, whereas in Côte d'Ivoire, the maximum threshold is 5 dB/Km [40]. The second main finding of this research is that rain is the main factor reducing FSO link quality in Côte d'Ivoire, and not fog as in London [41]. The rainy season is the least advantageous period for using an FSO link. In fact, during this period, the conditions favor the development of factors that lead to greater absorption, such as rain and fog. The stratification study revealed that Côte d'Ivoire is an environment with low turbulence instability. The results obtained in terms of reduction due to fog follow the same trend observed at Akure [8] and Kimberley in South Africa [40]. Indeed, the results obtained in these environments indicate that the reduction caused by fog decreases as the visibility distance increases, and that for a wavelength of 1550 nm, the maximum reduction is around 10 dB/Km [25]. The main difference in terms of visibility between our test areas and Akure and Kimberley is that, in Akure, visibility can reach 33.3 Km and 40 Km for Kimberly, while in Côte d'Ivoire, more precisely in Korhogo, Man, Bouaké, Bondoukou and Abidjan, the average visibility distance observed is 10

Km. For a mountainous setting such as Kimberly, the maximum degree of reduction observed is 0.11 dB/Km, while for Man it is 0.162 dB/Km [40]. Generally speaking, based on the results obtained, it can be stated that to achieve good results with an FSO connection in Côte d'Ivoire, it is advisable to favor connection distances of less than 4.5 km, and that the north presents the best profile for the deployment of an FSO link. However, for an excellent level of connectivity in a telecoms application, especially for a Fronthaul link, it is essential to find ways of improving link performance to reduce latency, and to use a stand-alone error correction system to improve the BER.

5 Conclusion

In a context where research into improving the performance of fifth-generation connectivity systems is booming, free-space atmospheric communication systems are taking root in telecommunications networks as a backhaul technology, offering exceptional throughput capabilities, low latency, high reliability and high cost-effectiveness. The aim of this study was to evaluate the performance of an FSO link in the context of setting up a telecommunications network in meteorological conditions such as Abidjan, Bouaké, Korhogo, Bondoukou and Man. The parameters taken into account included rain, fog, temperature and humidity. The analysis revealed that rain is the factor with the greatest impact on FSO link performance in each of our environments, and that the rainy season is the least suitable for its use in the Côte d'Ivoire meteorological context. Evaluation of the signal-to-noise ratio and the bit error rate in the presence of atmospheric attenuation factors showed that the link can continue to operate correctly over a distance of less than 4.5 km, with signal-to-noise ratio levels above 20 dB and bit error rate levels below 10^{-4} for Abidjan, Bouaké, Bondoukou, and below 10^{-6} for Korhogo. In terms of FSO link performance, the Man environment shows the weakest results, with BER levels above 10^{-3}. In order to improve the performance of the Ivorian Internet infrastructure using FSO technology, it is also essential to find techniques for improving the performance of this technology in the Ivorian environment. Some studies, notably that carried out by Abu Bakarr Sahr Brima, Edwin Ataro and Aladji Kamagate, have shown that acting on the polarisation state of light can have a significant impact on the performance of FSO systems [42]. In a forthcoming study, we intend to analyse the impact of using light polarisation states as a beam modulation scheme on improving the performance of FSO systems in Côte d'Ivoire.

References

1. Mheidly, N., Fares, M.Y., Fares, J.: Coping with stress and burnout associated with telecommunication and online learning. Front. Public Health **8**, 672 (2020)
2. World Bank data page. https://donnees.banquemondiale.org/?name_desc=true. Accessed 12 Aug 2023

3. Capri, R.: Telecommunications et croissance economique: Le cas de la telephonie Mobile en Cote D'ivoire. IOSR. J. Econ. Finan. (IOSR-JEF) **11**(2), 45–82 (2020)
4. Jahid, A., Alsharif, M.H., Hall, T.J.: A contemporary survey on free space optical communication: potentials, technical challenges, recent advances and research direction. J. Netw. Comput. Appl. **200**, 103311 (2022)
5. Shi, Y., Armghan, A., Ali, F., Aliqab, K., Alsharari, M.: Enriching capacity and transmission of hybrid WDM-FSO link for 5G mobility. Photonics **10**, 121 (2023). https://doi.org/10.3390/photonics10020121
6. Ghoname, S., et al.: Performance analysis of FSO communication system: Effects of fog, rain and humidity. In: 2016 Sixth International Conference on Digital Information Processing and Communications (ICDIPC). IEEE (2016)
7. Ajewole, M.O., Owolawi, P.A., Ojo, J.S., Adetunji, R.M.: Fog and rain attenuation characterization and performance of terrestrial free space optical communication in Akure, Nigeria. Aptikom J. Comput. Sci. Inf. Technol. **4**(3), 125–134 (2019)
8. Kone, D., Bamba, A., Kamagate, A.: FSO link based in Abidjan under weather conditions, in press (2023)
9. Andrews, L.C., Phillips, R.L.: Laser Beam Propagation Through Random Media, 2nd edn. Laser Beam Propagation Through Random Media (2005)
10. Ansari, I.S., Yilmaz, F., Alouini, M.S.: Performance analysis of FSO links over unified Gamma-Gamma turbulence channels. In: 2015 IEEE 81st Vehicular Technology Conference (VTC Spring), pp. 1–5. IEEE (2015)
11. Trichili, A., Cox, M.A., Ooi, B.S., Alouini, M.S.: Roadmap to free space optics. JOSA B **37**(11), A184–A201 (2020)
12. Estarán, J.M., Pointurier, Y., Bigo, S.: FSO SpaceComm links and its integration with ground 5G networks. In: Optical Fiber Communications Conference and Exhibition (OFC). San Diego, CA, USA 2019, pp. 1–3 (2019)
13. Sahoo, P., Yadav, A.: A comprehensive road map of modern communication through free-space optics. J. Opt. Commun., 000010151520200238. https://doi.org/10.1515/joc-2020-0238 (2020)
14. Hossain, M.F., Mahin, A.U., Debnath, T., Mosharrof, F.B., Islam, K.Z.: Recent research in cloud radio access network (C-RAN) for 5G cellular systems-A survey. J. Netw. Comput. Appl. **139**, 31–48 (2019)
15. Dhasarathan, V., Singh, M., Malhotra, J.: Development of high-speed FSO transmission link for the implementation of 5G and internet of things. Wireless Netw. **26**, 2403–2412 (2020)
16. Kiasaleh, K.: Channel estimation for FSO channels subject to Gamma-Gamma turbulence. In: Proceedings of the ICSOS, pp. 1–7 (2012)
17. Majumdar, A.K.: Advanced Free Space Optics (FSO). SSOS, vol. 186. Springer, New York (2015). https://doi.org/10.1007/978-1-4939-0918-6
18. Ghassemlooy, Z., Popoola, W., Rajbhandari, S.: Optical Wireless Communications: System and Channel Modelling with Matlab®. CRC press (2019)
19. Chaleshtory, Z.N., Gholami, A., Ghassemlooy, Z., Sedghi, M.: Experimental investigation of environment effects on the FSO link with turbulence. IEEE Photonics Technol. Lett. **29**(17), 1435–1438 (2017)
20. Zhang, H., et al.: February. Performance analysis of FSO system with different modulation schemes over gamma-gamma turbulence channel. In: 17th International Conference on Optical Communications and Networks (ICOCN2018), vol. 11048, pp. 191–197. SPIE (2019)
21. Gradstein, I.S., Ryzhik, I.M.: Table of Integrals, Series, and Products, 7th edn. (2007)

22. The wolfram functions site: ERFC functions. http://functions.wolfram.com/PDF/Erfc.pdf. Accessed 12 Aug 2023
23. The wolfarm functions site: MeijerG functions. http://functions.wolfram.com/PDF/MeijerG.pdf
24. Kottek, M., et al.: World map of the Köppen-Geiger climate classification updated (2006)
25. Weather data bank homepage. https://historique-meteo.net
26. Official open data portal CI. https://www.ins.ci/RGPH2021/RESULTATS%20DEFINITIFSRP21.pdf
27. Soro, G.E., et al.: "Estimation des pluies journalières extrêmes supérieures à un seuil en climat tropical: cas de la Côte d'Ivoire." Physio-Géo. Géographie physique et environnement **10**,211–227 (2016)
28. Kouadio, Y.K., Ochou, D.A., Servain, J.: Tropical Atlantic and rainfall variability in Côte d'Ivoire. Geophys. Res. Lett. **30**5, 4 (2003)
29. KEENETIC ADSL présentation page. https://help.keenetic.com/hc/en-us/articles/360002830880-ADSL-line-parameters. Accessed 12 Aug 2023
30. Forin, D.M., Incerti, G.: Free Space Optical Technologies: Trends in Telecommunications Technologies, ed. Bouras, Ch. J. (2010)
31. Yasir, S.M., Abas, N., Rauf, S., Chaudhry, N.R., Saleem, M.S.: Investigation of optimum FSO communication link using different modulation techniques under fog conditions. Heliyon, **8**(12), e12516 (2022)
32. Esmail, M.A., Fathallah, H., Alouini, M.S.: Outdoor FSO communications under fog: attenuation modeling and performance evaluation. IEEE Photonics J. **8**(4), 1–22 (2016)
33. Wallace, J.M., Hobbs, P.V.: Atmospheric Science: An Introductory Survey, vol. 92. Elsevier (2006)
34. Canut, G.: Intéraction Mousson/Harmattan, échanges de petite échelle (Doctoral dissertation, Université Paul Sabatier-Toulouse III) (2010)
35. Nauenberg, M.: Atmospheric refraction predictions based on actual atmospheric pressure and temperature data. Publ. Astron. Soc. Pac. **129**(974), 044503 (2017)
36. Grachev, A.A., Andreas, E.L., Fairall, C.W., Guest, P.S., Persson, P.O.G.: The critical Richardson number and limits of applicability of local similarity theory in the stable boundary layer. Bound. Layer Meteorol. **147**, 51–82 (2013)
37. Bouche-cousu blog, Wifi presentation page. https://bouchecousue.com/blog/comment-lire-la-force-dun-signal-wifi/. Accessed 12 Aug 2023
38. Rec. UIT-R S.522-5. https://www.itu.int/dms_pubrec/itu-r/rec/s/R-REC-S.522-5-199409-I!!PDF-F.pdf. Accessed 19 Aug 2023
39. Recommandation UIT-T G.997.1, série G: systèmes et supports de transmission, systèmes et réseaux numériques
40. Kolawole, O.O., Afullo, T.J., Mosalaosi, M.: Terrestrial free space optical communication systems availability based on meteorological visibility data for South Africa. SAIEE Africa Res. J. **113**(1), 20–36 (2022)
41. Nafees, M., Huang, S., Thompson, J., Safari, M.: Backhaul-aware user association and throughput maximization in UAV-aided hybrid FSO/RF network. Drones **7**(2), 74 (2023)
42. Brima, A.B.S., Ataro, E., Kamagate, A.: Performance enhancement of an FSO link using polarized quasi-diffuse transmitter. Heliyon **7**(11), e08248 (2021)